[7] A. Elsherbini and K. Sarabandi, "Very low-profile top-loaded UWB coupled sectorial loops antenna," *IEEE Antennas Wireless Propag. Lett.*, vol. 10, pp. 800–803, Aug. 2011.
[8] N. Behdad, M. Li, and Y. Yusuf, "A very low-profile, omnidirectional, ultrawideband antenna," *IEEE Antennas Wireless Propag. Lett.*, vol. 12, pp. 280–283, Mar. 2013.
[9] J.-F. Zürcher, "Tripod omnidirectional low profile antenna: A vertically polarized antenna with 90% bandwidth," *Microw. Opt. Technol. Lett.*, vol. 55, pp. 516–521, 2013.
[10] S. Abadi and N. Behdad, "An electrically small, vertically polarized ultrawideband antenna with monopole-like radiation characteristics," *IEEE Antennas Wireless Propag. Lett.*, vol. 13, pp. 742–745, Apr. 2014.
[11] M. Koohestani, J.-F. Zürcher, A. Moreira, and A. Skrivervik, "A novel, low-profile, vertically-polarized UWB antenna for WBAN," *IEEE Trans. Antennas Propag.*, vol. 62, no. 4, pp. 1888–1894, Apr. 2014.
[12] K. Ghaemi and N. Behdad, "A low-profile, vertically-polarized ultrawideband antenna with monopole-like radiation characteristics," *IEEE Trans. Antennas Propag.*, vol. 63, no. 8, pp. 3699–3705, Aug. 2015.
[13] A. Lai, K. Leong, and T. Itoh, "Infinite wavelength resonant antennas with monopolar radiation pattern based on periodic structures," *IEEE Trans. Antennas Propag.*, vol. 55, no. 3, pp. 868–876, Mar. 2007.
[14] T. Kaufmann and C. Fumeaux, "Low-profile magnetic loop monopole antenna based on a square substrate-integrated cavity," *Int. J. Antennas Propag.*, vol. 2015, 6 p., 2015, Art. no. 694385.
[15] D. Herold, L. Griffiths, and T. Y. Fung, "Lightweight, high-bandwidth conformal antenna system for ballistic helmets," in *Proc. IEEE Mil. Commun. Conf. (MILCOM)*, Oct. 2007, pp. 1–6.
[16] T. Björninen and F. Yang, "Low-profile head-worn antenna with a monopole-like radiation pattern," *IEEE Antennas Wireless Propag. Lett.*, vol. 15, pp. 794–797, Aug. 2015.
[17] M. Niroo-Jazi and T. Denidni, "A new triple-band circular ring patch antenna with monopole-like radiation pattern using a hybrid technique," *IEEE Trans. Antennas Propag.*, vol. 59, no. 10, pp. 3512–3517, Oct. 2011.

High-Efficiency Stacked Shorted Annular Patch Antenna Feed for Ku-Band Satellite Communications

Zhenchao Yang, Kyle C. Browning, and Karl F. Warnick

***Abstract*—Reflector-based satellite communication (SatCom) terminals require high sensitivity to minimize overall antenna size, and in view of their simplicity and high radiation efficiency, horn antennas are used almost exclusively as reflector feeds. As these terminals become more complex, smaller and more compact feeds that can be directly integrated with microstrip circuits are desirable. Standard microstrip antennas (MSAs) have unacceptably low radiation efficiency for use as reflector feeds. We show that the stacked shorted annular patch (SSAP) can be used as a replacement for horn feeds and achieves higher radiation and spillover efficiencies than conventional patch antennas due to the absence of distribution networks and dielectric substrates. Using a half-wavelength stacked patch as a director realizes a pattern that achieves high illumination efficiency with standard parabolic reflector geometries. Simulation and measurements show that the compact SSAP may be the first reported nonwaveguide feed antenna to achieve sensitivity comparable to that of a conventional horn feed.**

***Index Terms*—Antenna efficiency, compact antenna feed, satellite communications, stacked shorted annular patch.**

I. Introduction

Microstrip patch antennas are attractive for satellite communication (SatCom) applications due to low cost, low profile, and ease of fabrication. With careful substrate selection, high-efficiency microstrip patch arrays can be designed to serve as feeds for parabolic reflectors with performance nearly as good as traditional horn feeds and much smaller size and weight [1]. To achieve radiation efficiency comparable to a horn feed, low-loss PTFE-based substrate must be used. This material is relatively expensive and requires special processes during PCB fabrication. The efficiency of microstrip patch array feeds is also reduced by the distribution network, and surface waves launched by patch elements on the substrate surface and unwanted radiation from transmission lines can decrease spillover efficiency. For these reasons, an improved patch antenna design is desirable for use as a compact lightweight low-cost reflector feed.

Efficiency can be increased by eliminating transmission lines and exciting the antenna's radiating structures using spatial coupling. One approach is to arrange coplanar parasitic patches around the driven patch and driving them through tight edge coupling [2]. This improves efficiency, but the antenna gain is not high enough to illuminate a dish efficiently. Another approach is to utilize natural power spreading via surface wave modes. In [3], planar circularly symmetric electromagnetic band gap (PCS-EBG) structures were used to direct the surface wave to radiate constructively across a large aperture with the substrate surface serving as the transmission line. The excited surface waves were not axially symmetric, leading to different E-plane and H-plane patterns and poor reflector illumination. A PCS-EBG-based

Manuscript received October 08, 2015; revised January 05, 2016; accepted February 20, 2016. Date of publication April 06, 2016; date of current version May 30, 2016. This work was supported by the Research Grant from Linear Signal, LLC, Provo, UT, USA.

The authors are with the Department of Electrical and Computer Engineering, Brigham Young University, Provo, UT 84602 USA (e-mail: yzcown@gmail.com; kcbrowning@gmail.com; warnick@ee.byu.edu).

Color versions of one or more of the figures in this communication are available online at http://ieeexplore.ieee.org.

Digital Object Identifier 10.1109/TAP.2016.2551258

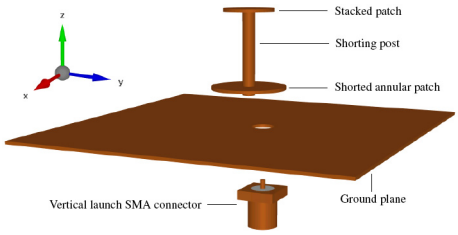

Fig. 1. Exploded view of the SSAP antenna feed.

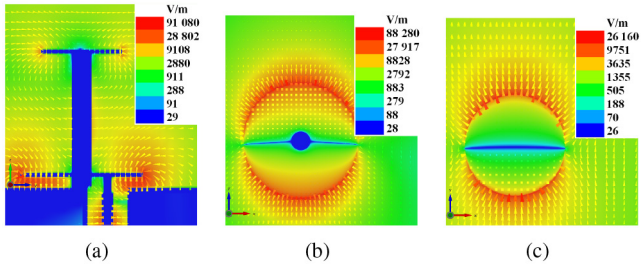

Fig. 2. E-field distribution at 12 GHz. (a) Cross-sectional view on a yz-plane. (b) xy-plane on the SAP. (c) xy-plane on the top patch. The distributions show the two patches working in the same mode with 180° phase difference.

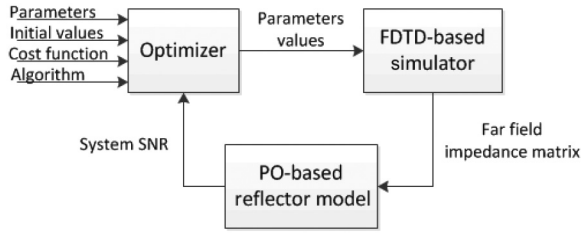

Fig. 3. Optimization flow chart for on-reflector simulation and feed design tuning.

feed antenna would also be relatively large in size, leading to undesirable reflector blockage. These aperture-coupled antennas can provide low loss, but for use as reflector feeds, higher gain and improved illumination patterns are needed.

Further improvements to gain and aperture efficiency while maintaining the low loss of a spatially coupled aperture are difficult to achieve and require a creative design. While most high gain antennas are arrays or other laterally extended structures that require lossy interconnects, gain can also be enhanced by increasing the axial extent of the antenna. This type of gain enhancement has been realized using dielectric superstrates, Fabry–Perot cavities, stacked EBG layers, and various types of lenses, but these techniques generally suffer from poor radiation efficiency and high fabrication cost, making them unsuitable as SatCom reflector feeds.

A compact high-gain antenna was proposed for small satellite applications in [4], but the aperture-coupling feed technique is not the most efficient way to feed a microstrip patch antenna [5]. In addition, the high-gain antenna was directly integrated on a low earth orbit satellite to serve as a primary antenna. This letter provides a high-efficiency feed antenna design for Ku-band SatComs based on the stacked shorted annular patch (SSAP) structure with direct probe feeding. Our proposed feed antenna resolves the aforementioned issues and realizes high radiation efficiency and high gain in a compact structure.

II. Antenna Design

The feed antenna design combines both lateral and vertical extensions into a circular microstrip antenna (MSA) to achieve high gain, high efficiency, and low sidelobes. The shorted annular patch (SAP) antenna was developed in [6] to eliminate surface waves for microstrip patch antennas. By arranging a parasitic coupled patch in a right distance from the main patch, higher gain can be achieved [4], [7]. Air substrate was used to mitigate surface wave and eliminate dielectric loss. The shorting post is located at the centers of the patches where the current of the dominant radiating mode TM_{11} is negligible and acts merely as mechanical support. As a result, the primary patch diameter is approximately half the free space wavelength at 12 GHz. The resulting SSAP feed design is shown in Fig. 1.

Matching the SSAP was accomplished by adjusting the radius of the main circular patch and the feed pin location like a normal patch design. As a dish feed, the pattern shape needs to be optimized for high aperture and spillover efficiency as well, which is mainly determined by the distance between patches and the radius of the parasitic patch. Using the model described in Section III, the design was optimized for the maximum signal-to-noise ratio (SNR) when connected to a low noise amplifier and used as a receiving feed for a parabolic reflector. The parasitic patch maximizes the antenna gain at around half-wavelength distance, which is related to the directors in a Yagi-Uda antenna but at a different spacing. To demonstrate the radiating mechanism, E-fields around the optimized SSAP on different planes are plotted in Fig. 2. The cross-sectional view in Fig. 2(a) shows the top patch reradiates based on its fringe field with opposite direction of the main patch E-field. Fig. 2(b) and (c) further shows that the two patches work in the same mode but with 180° phase difference. Considering the half-wavelength distance between the patches, the SSAP can be treated as an end-fire array of patch antennas with two elements.

A direct probe feed from a subminiature version A (SMA) connector or RF circuitry to the SAP was used in the prototype, but could readily be replaced with a transmission line feed or direct connection to a low-noise amplifier in a final design. The design uses only a single-layer PCB and retains its high efficiency even with low-cost, low-quality substrates.

At Ku-band, besides linearly polarized free-to-air (FTA) signals, circularly polarized direct broadcasting service (DBS) signal is also provided. To receive DBS signals, a hybrid and the second orthogonal linearly polarized port are needed to create dual circular polarizations [8]. The SSAP can be easily fabricated on the ground of the hybrid.

III. Simulation and Measurement Results

To optimize the SSAP structure for the best illumination pattern as a reflector feed antenna, primary patterns were simulated first within an FDTD-based simulator (EMPIRE, IMST GmbH), and then secondary patterns reflected from the dish were calculated by the physical optics (PO) approximation using an in-house code. Spillover noise, sky noise, and electronics were included in the PO model to estimate the overall system SNR [9]. This hybrid model was then embedded in an optimizer, and the design was tuned to maximize the overall system SNR as shown in Fig. 3. The optimized SSAP configuration for a parabolic dish with a 0.6 focal length to diameter ratio (f/D) is illustrated in Fig. 4.

The simulated and measured S-parameters agree well as shown in Fig. 5. The simulated −10-dB reflection bandwidth is 480 MHz, which approximately covers the whole FTA band from 11.7 to 12.2 GHz. The deviation between measurement and simulation of S_{11} is caused by fabrication and assembly errors. Hand assembly leads to inaccuracies in the geometry such as a tilt of the fabricated spool relative to the ground plane and misalignment of the SMA connector with the center

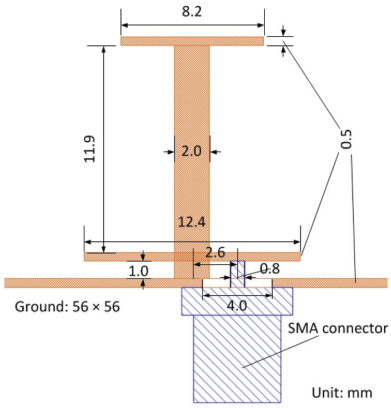

Fig. 4. Side view of the SSAP antenna feed.

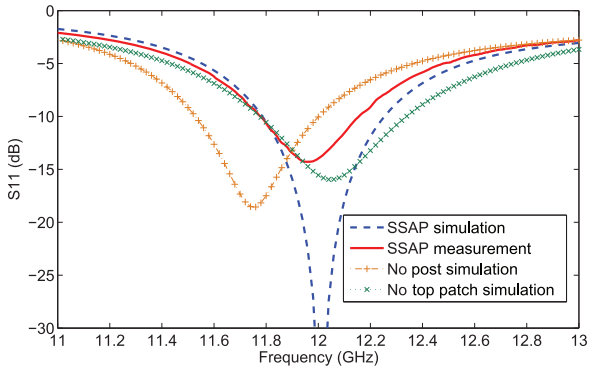

Fig. 5. Simulated and measured return loss of the SSAP antenna, compared with the simulated cases of no shorting post and no top patch.

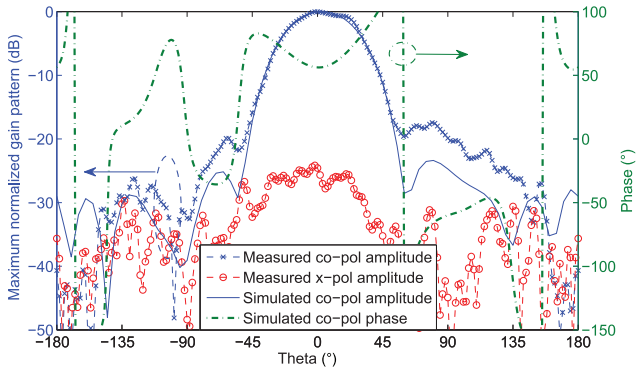

Fig. 6. E-plane radiation amplitude and phase patterns of the SSAP at 12 GHz.

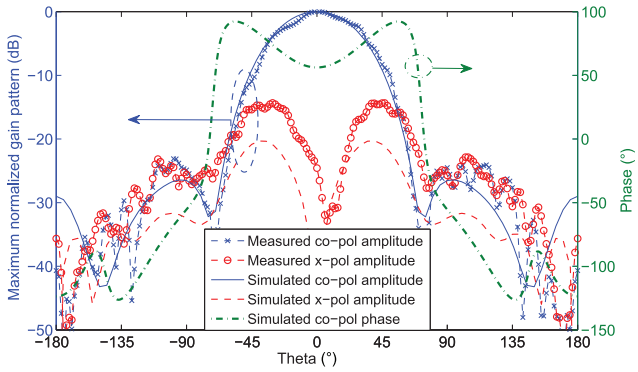

Fig. 7. H-plane radiation amplitude and phase patterns of the SSAP on at 12 GHz.

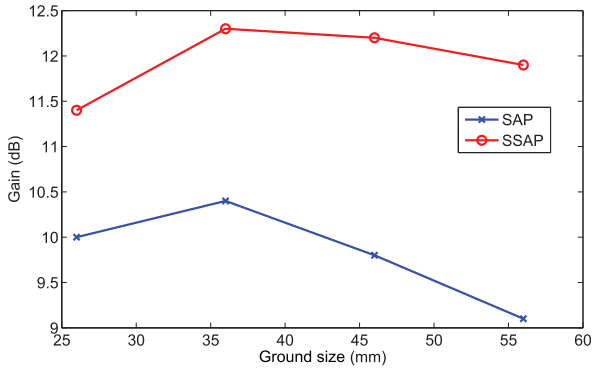

Fig. 8. Gain of SAP and SSAP as a function of ground plane size.

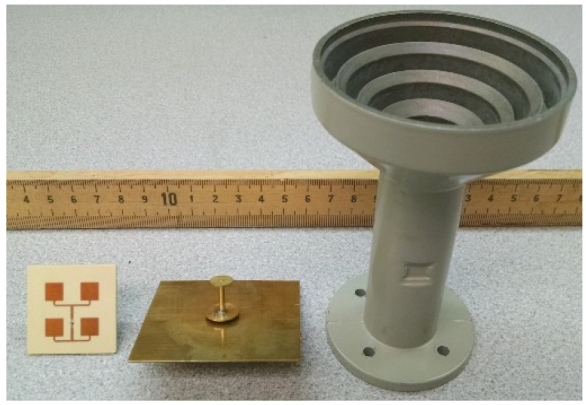

Fig. 9. Fabricated 2×2 MSA and SSAP feeds shown in comparison to the commercial horn feed used in experimental tests. The size advantage of the SSAP feed is readily apparent.

of the hole on the ground. In addition, the cases with no shorting post and no top patch are simulated as well, and the S-parameter results are included in Fig. 5. This shows that the shorting post only causes a small resonant frequency shift due to the current disturbance and the top patch does not affect the impedance match significantly. As a result, all methods capable of enhancing bandwidth for patch antennas can be applied to the SSAP. Multiple stacked patches or coupling feed are promising techniques [10], [11].

Simulated and measured radiation patterns in the E-plane and H-plane are shown in Figs. 6 and 7, respectively. The patterns were measured using a near-field scanner system. The simulated radiation patterns show a −8-dB taper at the dish rim and only −23-dB highest sidelobe level, which implies good spillover performance. The phase patterns show stable phase distribution across the main beam range. The SSAP gain is stable as the ground size varies as shown in Fig. 8, so smaller ground can be used if the space requirement is strict. The SSAP gain at 56-mm ground size is 3 dB higher than that of SAP, verifying the radiating mechanism explained in Section III.

SNR measurement for a typical 90-cm offset parabolic reflector pointing at Galaxy 19 fed by the proposed feed antenna was carried out using a Super Buddy satellite signal level meter (Applied Instruments, Inc.). The dish has an offset angle 25° and an opening angle equivalent to a symmetric reflector with a f/D of 0.74. A horn feed and a MSA-array feed consisting of 2 × 2 square patches [1] were also simulated and measured in the same setups. The three feed antennas are compared side by side in Fig. 9. The modeled horn was somewhat

TABLE I
EFFICIENCY AND SNR RESULTS OF DIFFERENT ANTENNA FEEDS AT 12 GHZ ON AN F/D = 0.74 DISH

Antenna feed	η_{ap} (%)	η_{sp} (%)	η_{rad} (%)	SNR_{sim} (dB)	SNR_{meas} (dB)
MSA	62	70	93	11.8	9.5
SSAP	75	84	98	14.3	12.6
Horn	76	92	98	15.2	13.3

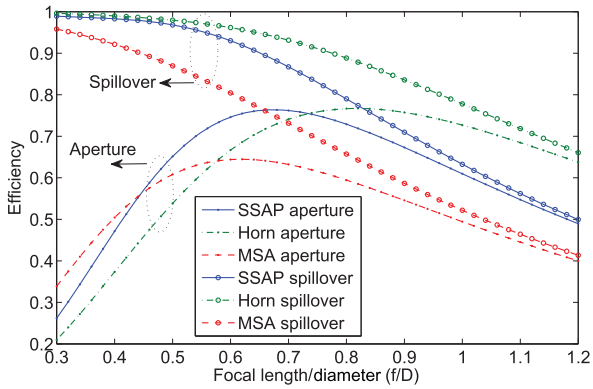

Fig. 10. Simulated aperture, spillover, and radiation efficiencies of three types of feed as a function of f/D.

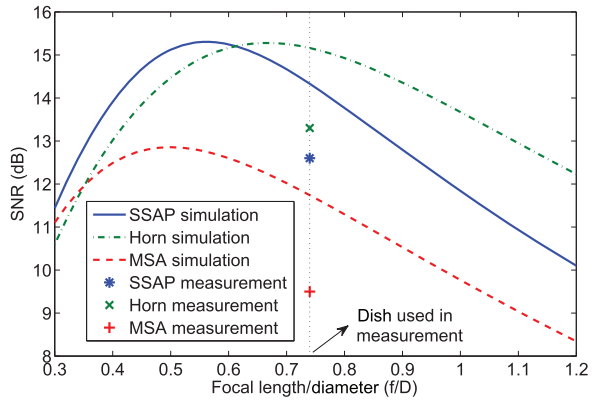

Fig. 11. Simulated SNR of three types of feed as a function of f/D. Measured values on an f/D = 0.74 dish.

simplified compared to the actual horn but was qualitatively similar in function. Table I lists the efficiencies and simulated and measured SNR at 12 GHz. The measured SNR agrees well with simulation in relative value between each feed type. The absolute difference in the measured and simulated SNR values is caused by unmodeled effects including feed support scattering, mispointing, atmospheric attenuation, and uncertainty in the satellite transponder EIRP. The measured SNR fluctuates over a 4-dB range depending on outdoor weather and environmental conditions. As a result, the small absolute difference with respect to the simulations is unimportant.

The measured SNR for the SSAP feed was 3 dB higher than the MSA feed and only 0.7 dB lower than the horn. Due to the absence of lossy distribution networks and dielectric substrates, the intrinsic radiation efficiency of the SSAP is likely to be as high as that of the horn feed. The measured SNR value for the SSAP feed was reduced by an additional test connector not used in the horn feed setup. The additional connector loss was 0.2 dB, corresponding to roughly 0.5-dB reduction in SNR. Without this connector, the difference between the actual horn and SSAP performance would be negligible.

Both SSAP and MSA feeds were optimized for a symmetric reflector with a 0.6 f/D. Tests were done with a 0.74-f/D dish, which means that the reflector has a lower opening angle and the spillover efficiency is lower than that of the optimal reflector geometry. To demonstrate that the performance of the SSAP is better for dishes with smaller f/D and wider opening angle, the efficiencies and SNR of the three feeds were simulated as a function of f/D as shown in Figs. 10 and 11. The SSAP performs best on an f/D = 0.56 dish with both efficiencies and SNR comparable to the best horn-fed dish. The MSA feed is poorer over all f/D values due to its higher sidelobe level and a flatter illumination pattern. By eliminating surface waves and introducing a director, the SSAP overcomes those difficulties and produces a highly efficient illumination pattern.

IV. CONCLUSION

An SSAP antenna was designed and optimized as a parabolic reflector feed for Ku-band SatComs. The feed is lighter and simpler than a traditional horn feed. Without distribution networks and dielectric substrates, the antenna loss is lower than that of MSA feeds, and spurious radiation from transmission lines and surface waves is eliminated completely, leading to high radiation efficiency. The half-wavelength stacked patch increases the gain and shapes the pattern to illuminate a standard Ku-band SatCom dish efficiently. The overall SNR performance is only 0.7 dB lower than a commercial horn feed, as verified by simulation and measurement on an f/D = 0.74 parabolic reflector. The SSAP is optimal for a dish with $f/D = 0.56$ and matches the best horn performance for that geometry. To our knowledge, this SSAP is the first reported nonhorn feed antenna that achieves performance comparable to a horn feed.

Future work includes dual circularly polarized and wideband variations of the SSAP feed.

ACKNOWLEDGMENT

The authors would like to thank T. Shahvirdi and Prof. R. Baktur at Utah State University for helping measure the antenna patterns.

REFERENCES

[1] Z. Yang, K. F. Warnick, and C. L. Holloway, "A high radiation efficiency microstrip array feed for Ku band satellite communication," in *Proc. IEEE Antennas Propag. Soc. Int. Symp. (APSURSI'13)*, 2013, pp. 1576–1577.
[2] R. Q. Lee, R. Acosta, and K. F. Lee, "Radiation characteristics of microstrip arrays with parasitic elements," *Electron. Lett.*, vol. 23, no. 16, pp. 835–837, 1987.
[3] N. Llombart, A. Neto, G. Gerini, and P. de Maagt, "Planar circularly symmetric EBG structures for reducing surface waves in printed antennas," *IEEE Trans. Antennas Propag.*, vol. 53, no. 10, pp. 3210–3218, Oct. 2005.
[4] E. Arnieri, L. Boccia, G. Amendola, and G. Di Massa, "A compact high gain antenna for small satellite applications," *IEEE Trans. Antennas Propag.*, vol. 55, no. 2, pp. 277–282, Feb. 2007.
[5] D. M. Pozar and B. Kaufman, "Comparison of three methods for the measurement of printed antenna efficiency," *IEEE Trans. Antennas Propag.*, vol. 36, no. 1, pp. 136–139, Jan. 1988.
[6] D. R. Jackson, J. T. Williams, A. K. Bhattacharyya, R. L. Smith, S. J. Buchheit, and S. A. Long, "Microstrip patch designs that do not excite surface waves," *IEEE Trans. Antennas Propag.*, vol. 41, no. 8, pp. 1026–1037, Aug. 1993.
[7] R. Q. Lee and K. F. Lee, "Experimental study of the two-layer electromagnetically coupled rectangular patch antenna," *IEEE Trans. Antennas Propag.*, vol. 38, no. 8, pp. 1298–1302, Aug. 1990.
[8] Z. Yang and K. F. Warnick, "Multiband dual-polarization high-efficiency array feed for Ku/Reverse-band satellite communications," *IEEE Antennas Wireless Propag. Lett.*, vol. 13, pp. 1325–1328, Jul. 21, 2014.

[9] K. F. Warnick, D. Carter, T. Webb, J. Landon, M. Elmer, and B. D. Jeffs, "Design and characterization of an active impedance matched low-noise phased array feed," *IEEE Trans Antennas Propag.*, vol. 59, no. 6, pp. 1876–1885, Jun. 2011.
[10] S. Egashira and E. Nishiyama, "Stacked microstrip antenna with wide bandwidth and high gain," *IEEE Trans. Antennas Propag.*, vol. 44, no. 11, pp. 1533–1534, Nov. 1996.
[11] K. L. Lau and K. M. Luk, "A novel wide-band circularly polarized patch antenna based on L-probe and aperture-coupling techniques," *IEEE Trans. Antennas Propag.*, vol. 53, no. 1, pp. 577–582, Jan. 2005.

Microfluidically Reconfigured Wideband Frequency-Tunable Liquid-Metal Monopole Antenna

Abhishek Dey, Rasim Guldiken, and Gokhan Mumcu

***Abstract*—A microfluidically reconfigured wideband frequency-tunable liquid-metal monopole antenna is presented. The antenna operation relies on continuous moving of the liquid-metal volume over the capacitively coupled microstrip line feed network with a micropump unit. To maximize the capacitive coupling at the feed point, the antenna is realized by bonding microfluidic channel molds prepared in polydimethylsiloxane (PDMS) polymer with 1-mil-thick liquid crystal polymer (LCP) substrate. The concept is demonstrated through the design and experimentation of a 4:1 frequency-tunable monopole antenna that operates from 1.29 to 5.17 GHz. The presented monopole antenna can also be utilized as an element to form wideband frequency-tunable high-gain antenna apertures without necessitating any additional micropump units. This is accomplished by resorting to strategically meandered or interconnected microfluidic channels. This concept is demonstrated through the design and experimentation of a 4×1 microfluidically controlled monopole array capable of providing 2:1 frequency tuning range from 2.5 to 5 GHz.**

***Index Terms*—Frequency reconfigurable antenna, liquid metal, microfluidics, monopole.**

I. Introduction

The demanding size reduction needs of multifunctional communication systems have generated interest in reconfigurable antenna technologies. Recent literature has extensively investigated the reconfiguration capabilities offered by varactors [1], PIN diodes [2], ferroelectric varactors [3], microelectromechanical systems (MEMS) switches, and MEMS capacitors [4]. These techniques are well recognized to offer compact and cost-effective high-reconfiguration speed antennas. However, they continue to exhibit drawbacks in terms of several RF performance metrics such as the range of frequency tunability, power handling capability, and radiation efficiency. Microfluidic-based reconfigurable antennas have been shown to be promising for addressing these needs [5]. For example, stretchability of the liquid metal-filled polymer substrates has been demonstrated for frequency-tunable and -flexible antennas [6]. Loading of antenna substrates with different type of liquids exhibiting diverse permittivity values has been proposed for frequency reconfigurability [7]. A continuously movable liquid-metal slug inside plastic tubing has been used as a parasitic director to generate beam steering from a circular loop antenna [8] and a frequency-tunable Yagi–Uda monopole array [9]. Microfluidically repositionable liquid-metal patch antennas have been utilized behind microwave lenses to generate beam-scanning mm-wave focal plane arrays [10]. In addition, repositioning of liquid metals inside microfluidic channels and tubes has been proposed for frequency-tunable filter [11] and frequency-selective surface implementations [12].

More recently, different from the aforementioned techniques, a liquid-metal monopole antenna that can dynamically change its length has been introduced [13]. Since liquid metals react with conventional metals used in printed circuit boards, a key enabler of this monopole antenna was the realization of its feeding mechanism with capacitive coupling. The high level of coupling between the microstrip feed line and the antenna was accomplished with microfluidic channels manufactured by bonding a 1-mil ($= 25.4$ μm)-thick low-loss liquid crystal polymer (LCP) substrate with a relatively thick (~ 2 mm) polydimethylsiloxane (PDMS) substrate. This communication presents a detailed investigation of this antenna concept by also enhancing the frequency tuning range to 4:1 (1.29–5.17 GHz) through a different feed coupling scheme. A system-level implementation with external micropumps is presented. Microfluidic channel dimensions are selected through detailed flow characterizations to achieve a high tuning speed with reliable liquid-metal volume movement. The antenna is shown to operate with a tuning speed of 242.5 MHz/s and exhibit > 1.3 dB measured realized gain across its frequency tuning range.

The presented antenna also allows for high-gain frequency-tunable antenna arrays operating within a wide frequency range. When resorted to meandered or interconnected microfluidic channels, the implementation of such arrays can be accomplished by using a single bidirectional micropump unit. To demonstrate this capability, in this communication, a 4×1 linear broadside array operating from 2.5 to 5 GHz is designed and experimentally verified. The array operates with measured > 6 dB broadside gain and a tuning speed of 125 MHz/s. This communication is organized as follows. Section II introduces the wideband frequency-tunable liquid-metal monopole-antenna concept and carries out an example design based on experimental microfluidic channel-flow characterizations. Section III provides the experimental verification of the antenna and details its operation with external micropumps. Section IV presents the 4×1 array to demonstrate realization of wideband frequency-tunable high-gain antenna arrays. Finally, Section V includes the concluding remarks.

II. Liquid-Metal Monopole

Fig. 1 depicts the reconfiguration principle and substrate stack-up of the liquid-metal monopole antenna. The liquid metal is enclosed inside a microfluidic channel fabricated within 2-mm-thick PDMS ($\varepsilon_r = 2.8$, $\tan\delta = 0.02$) using soft lithography process. The microfluidic channel is sealed using a 1-mil-thick (1 mil $= 0.001$ inches $= 25.4$ μm) Rogers Ultralam 3908 LCP-based substrate layer ($\varepsilon_r = 2.9$, $\tan\delta = 0.0025$). The LCP layer is bonded to a 62-mil-thick Rogers RT5880 substrate ($\varepsilon_r = 2.2$, $\tan\delta = 0.0009$) that carries the 50-Ω microstrip feed line and ground plane metallizations. The microfluidic channel is

Manuscript received September 30, 2014; revised January 02, 2016; accepted March 25, 2016. Date of publication April 06, 2016; date of current version May 30, 2016. This work was supported by the U.S. National Science Foundation under a CAREER award (ECCS-1351557).

A. Dey and G. Mumcu are with the Center for Wireless and Microwave Information Systems (WAMI), Department of Electrical Engineering, University of South Florida, Tampa, FL 33620 USA (e-mail: abhishek@mail.usf.edu).

R. Guldiken is with the Department of Mechanical Engineering, University of South Florida, Tampa, FL 33620 USA (e-mail: guldiken@usf.edu).

Color versions of one or more of the figures in this communication are available online at http://ieeexplore.ieee.org.

Digital Object Identifier 10.1109/TAP.2016.2551358